minerals

MDPI

Article

Mineral Inventory of the Algares 30-Level Adit, Aljustrel Mine, Iberian Pyrite Belt, Portugal

Teresa P. Silva [1,*], João X. Matos [2], Daniel De Oliveira [1], João P. Veiga [3], Igor Morais [2], Pedro Gonçalves [2] and Luís Albardeiro [2]

1 LNEG (National Laboratory for Energy and Geology), Mineral Resources and Geophysics Research Unit, Estrada da Portela, Apartado 7586, 2610-999 Amadora, Portugal; daniel.oliveira@lneg.pt

2 LNEG (National Laboratory for Energy and Geology), Mineral Resources and Geophysics Research Unit, Bairro de Val d'Oca, Apartado 14, 7601-909 Aljustrel, Portugal; joao.matos@lneg.pt (J.X.M.); igor.morais@lneg.pt (I.M.); pedro.goncalves@lneg.pt (P.G.); luis.albardeiro@lneg.pt (L.A.)

3 CENIMAT/I3N (Materials Research Centre), Materials Science Department, Faculty of Sciences and Technology, NOVA University of Lisbon, 2829-516 Caparica, Portugal; jpv@fct.unl.pt

* Correspondence: teresa.pena@lneg.pt

Received: 9 September 2020; Accepted: 24 September 2020; Published: 27 September 2020

Abstract: Mining activity in Algares (Aljustrel Mine, Portuguese sector of the Iberian Pyrite Belt, IPB) stems prior to Roman times. As the orebody is vertical and relatively thin, mining was carried out mainly along underground adits (galleries). Nowadays, the deposit is considered exhausted and the area is being rehabilitated for a different use. The Algares +30 level adit intersects two volcanic units of the IPB Volcano-Sedimentary Complex. The massive sulphide and related stockwork zone are hosted by the *Mine Tuff* volcanic unit and are exposed in the walls of the gallery, showing intense hydrothermal alteration. Along the mine adit, the geological sequence is affected by strong oxidation and supergene alteration, giving rise to the formation of secondary minerals through the oxidation of the sulphides. The most common minerals found were melanterite ($FeSO_4{\cdot}7H_2O$) and chalcanthite ($CuSO_4{\cdot}5H_2O$), forming essentially massive or crystalline aggregates, ranging from greenish to bluish colours. Melanterite from the walls revealed to be Cu-rich by opposition to that from stalactites/stalagmites formed below the old ore storage silo revealing the low-copper-grade ores exploited underground. The mineralogy of the efflorescent salts was used to ascertain the processes involved in their formation, and moreover, the inventory of minerals is presented, as well as their principal characteristics.

Keywords: efflorescent minerals; adit walls; stalactites/stalagmites; mineral inventory; Algares; Iberian Pyrite Belt mine; sulphide ores

1. Introduction

With more than 90 deposits of massive polymetallic sulphide ores, the Iberian Pyrite Belt (IPB) is one of the most important European metallogenic provinces [1,2]. Ten deposits (located in Portugal) can be considered large-sized with regards to their Cu-Zn-Pb contents, including the operating Neves-Corvo and Aljustrel mines. Pyrite (FeS_2) is the most common ore mineral. Roman mining practice focused on the exploitation of secondary ores (oxidation zone—iron cap and supergene alteration zone) and, in addition, of primary pyrite ore. The ore was roasted in place to extract the metals for export. Some of the Roman mines were very big endeavours and caused the first events of acid mine drainage (AMD) known in Portugal [3].

Mining activity in Algares (Aljustrel mine) occurred prior to the Roman Empire's occupation of the Iberian Peninsula. Vipasca Mine, as it was known when exploited during the Empire, was considered

one of the main mining centres [3,4]. As the Algares orebody is vertical and relatively thin, mining was never developed in open pit settings, allowing its preservation [5].

In the 19th century, modern exploration began mainly through wells or adits (galleries), reaching a depth of about 360 m [3,6–8]. Presently, the Algares deposit is considered exhausted and the area is being rehabilitated for mining and geological tourism. Aljustrel has a vast mining heritage, resulting mostly from the 19th-century mining activity, which is characterised by old mine structures (cementation tanks, mining headgears, pits, etc.) and underground adits [4,5].

The outcropping Algares deposit forms a NW–SE narrow gossan, mapped along 900 m [9–11]. This structure is classified as a natural geosite [12] considering the particular geological heritage associated with the erosion and supergene alteration of a VMS deposit [5,8,13]. To promote new educational visits, the Company Empresa de Desenvolvimento Mineiro (EDM) carried out recent mine rehabilitation inside the Algares +30 level adit (approximately 500 m long). Soon, thematic underground visits will be promoted by the Aljustrel Municipality included in the future Aljustrel Mining Park. Indeed, the oxidation/hydration of sulphides in moist air resulted in the formation of simple and complex multicoloured sulphates along the walls of the Algares +30 level adit, making it a natural mineralogical museum, attractive for underground visits in a geotourism context.

Since the 1990s, the Algares mine sector has been in a mine closure process [4]. During the mine rehabilitation project, the Algares mine gallery was cleaned and enlarged for public visits. Protection structures were constructed including wood pillars, concrete walls, and metallic networks. A new illumination system and a new public lift were constructed. Along the mine adit, a continuous air flow occurs adjusted in both dry and wet seasons. The continuous air flow and connection with old mine infrastructures like the ore mill (with barren brittle massive sulphides) and underground flooded mine galleries (e.g., Vipasca shaft) permit a continuous process of dissolution and open space mineral precipitation. New minerals are being formed in rock faces and in recent mine infrastructures like protective metallic nets, concrete walls, and iron ore distributors.

The first results of the mineral characterisation [14] performed on efflorescent materials revealed mainly the presence of both simple and complex sulphates with different degrees of hydration. Melanterite ($FeSO_4{\cdot}7H_2O$) and chalcanthite ($CuSO_4{\cdot}5H_2O$) are the most common minerals, forming essentially massive or crystalline aggregates, ranging from greenish to bluish colours.

An inventory of minerals found in the multi-coloured aggregates that cover the walls of the Algares +30 level is presented, as well as the foremost characteristics of the identified minerals (habit and colour), including those prevailing in stalactites/stalagmites. Furthermore, the mineralogy of the efflorescent salts was used to identify and understand the processes involved in their formation.

2. Geological Setting

The Aljustrel mining site has been related with the exploitation of mainly copper, lead and zinc. Gold and silver were by-products. It includes six independent ore lenses (Estação, Feitais, Algares, Moinho, São João and Gavião), as well as the Pedras Brancas Metallurgical Complex (approximately 10 km ESE of Aljustrel) [4,15–17]. The sulphide mineral assemblages of these orebodies consist mostly of pyrite (FeS_2) and minor amounts of sphalerite (ZnS), chalcopyrite ($CuFeS_2$), arsenopyrite (FeAsS), tetrahedrite [$(Cu,Ag)_{10}(Fe,Zn)_2Sb_4S_{13}$], galena (PbS), stannite (Cu_2FeSnS_4), pyrrhotite ($Fe_{1-x}S$) and some native bismuth [18]. Pyrite is the main sulphide (>90%). Based on the Feitais and Moinho petrography [18], copper is present in chalcopyrite and sulphosalts and in less abundant minerals such as bournonite, stannite, meneghinite and enargite [18]. According to this author, lead is present in galena, jamesonite, meneghinite, kobellite and plagionite, and zinc is present in sphalerite. Primary pyrite textures include colloformic, atoll and framboid structures. However, annealing related to ore recrystallisation, locally related to significant deformation, is common. Presently, only the Feitais and Moinho massive sulphide and stockwork ores are currently being mined by Almina Company.

The geology of the Aljustrel area is characterised by the occurrence of volcano-sedimentary sequences, consisting mostly of Tournaisian-age felsic volcanic rocks hosting the massive sulphide

deposits, capped by a set of jaspers unit, black, siliceous and purple shales and volcanogenic sediments of the Paraíso Formation (all defining the Volcano-sedimentary Complex, VSC), and subsequently overlain by a flysch sedimentary sequence (Mértola Formation) [15,16,19–21]. Minor mafic volcanism occurred in a submarine environment and the presence of ignimbritic flows suggests transient subaerial or extremely shallow water conditions [1]. The VSC in Aljustrel defines a NW–SE trending anticlinorium structure with subvertical rock and an ore lenses distribution. Above the aforementioned Palaeozoic stratigraphic sequence, a succession of Cenozoic-age fluvial and continental sediments mainly composed of sandstones, mudstones, conglomerates and carbonates were deposited, forming the Alvalade/Sado Basin [19].

The Algares adit intersects, from E to W, two volcanic units of the IPB's VSC, the *Megacrystal Tuff* unit (Vap in Figure 1) and the MT unit (*Tufo da Mina–Mine Tuff*) [15,16,19–21] (see the geological map in Figure 1). The massive sulphide and related stockwork zone are hosted by the *Mine Tuff* volcanic unit (Va in Figure 1) and are exposed on the walls of the underground adit, showing intense sericitic and chloritic hydrothermal alteration. Along the mine adit, this geological sequence is affected by intense weathering, giving rise to the formation of a natural mineralogical laboratory where secondary minerals are precipitated through the oxidation of the sulphides.

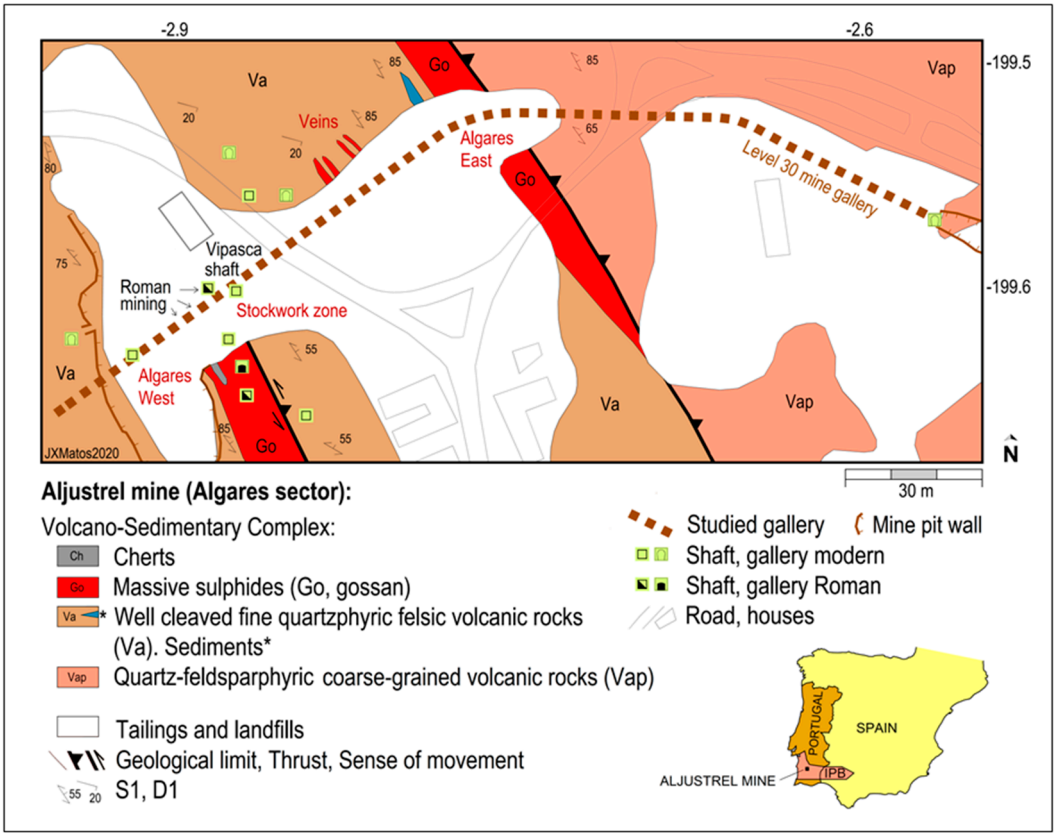

Figure 1. Geological map of the Aljustrel mine Algares NW sector. Level +30 mine gallery is projected at the surface. Minerals and crystals were collected in this gallery at Algares West and Algares East gossan orebodies and *Mine Tuff* volcanic unit rocks (Va) where stockwork veins occur. Old Vipasca Roman mine shafts and tunnels are visible in the studied gallery and on the surface. Coord. Hayford-Gauss Lisbon IPCC in km.

Two gossans were intersected: Algares East, located in the SW of the *Megacrystal Tuff* unit (tectonic shear zone contact), and Algares West, located near the Vipasca main shaft in the central sector of the *Mine Tuff* volcanic unit. Large stockwork zones outcrop in both sides of this ore lens. Each gossan was developed above the two massive sulphide ore lenses. The location of these structures and surface

mapping [9,15] suggest that the Algares West ore lens is compressed, probably in a narrow synform (Figure 1).

3. Materials and Methods

More than 100 georeferenced efflorescent samples were collected from the walls and roof of the Algares +30 level adit along its entire length, considering both colour and crystal morphology (Figures 1 and 2). Sampling was performed in September 2018 with a temperature of about 20 °C inside the adit. To prevent mineralogical changes of some unstable minerals, samples were preserved in closed containers and quickly analysed as soon as they reached the laboratory. Fragments for X-ray diffraction (XRD) were selected (approx. 200) using the stereomicroscope (Stemi SV-11, Zeiss, Jena, Germany), and images were collected with a digital Zeiss camera (Axio-Cam Mrc). Several images were mustered from the same fragment with the focus set at different levels, all of which were compiled together in Adobe Photoshop^{TM} using the focus stacking method.

Figure 2. Aspects of the coloured walls in the Algares +30 level adit (the blue is mainly chalcanthite), and green stalactites (melanterite) observed below the Algares ore storage silo.

Two XRD equipment were used, due to the large number of powdered (roughly comminuted, to avoid mineralogical changes) samples: (1) A Philips PW 1500 powder diffractometer with Bragg–Brentano geometry, equipped with a large-anode copper tube operating at 50 kV–40 mA and a curved graphite crystal monochromator; (2) a Rigaku Dmax III-C 3kW powder diffractometer with a Bragg–Brentano geometry, using Cu Kα radiation at 40 kV and 30 mA settings with a 20° to 65° 2θ range, an acquisition time of 1 s and a 2θ increment of 0.04°.

To corroborate XRD crystalline phase identification, thermo-analytical techniques—simultaneous differential thermal analysis (DTA) and thermogravimetry (TG)—were occasionally used, using a SETARAM 92-16.18 apparatus, incorporating a microbalance with a controlled argon gas flow (inert atmosphere). About 70–80 mg of milled sample was deposited in an alumina (α-Al_2O_3) crucible.

The reference material was alumina powder. Therefore, a DTA-TG assay was performed in one sample of supposedly chalcanthite, and the heating temperature ranged from ambient to 1000 °C at a heating rate of 10 °C min^{-1}. For the supposedly melanterite samples, the temperature interval was the same but at a heating rate of 17 °C min^{-1}.

The identification of some mineralogical phases proved to be difficult due to the solid solution between end-members of the sulphate-mineral groups or to the overlapping of peaks. For that reason, a portable X-ray fluorescence (p-XRF) equipment (Genius 9000 + 7000 from Skyray Instrument) was also used at the laboratory for a rapid chemical characterisation (elements below K could not be measured) of the powdered samples to help in the XRD identification, whenever necessary. Occasionally, for crucial magnesium content determination, a semi-quantitative chemical analysis was performed through X-ray fluorescence spectrometry with a wavelength-dispersive system (XRF-WDS), using a PANalytical 4.0 AXIOS sequential spectrometer (Rh X-ray tube) under He flow.

4. Results

4.1. Mineral Inventory of the Algares Adit

The mineralogical phases identified in efflorescence samples are listed in Table 1, in alphabetical order for easier reading, constituting a mineral inventory of the Algares adit. The mineral characterisation of secondary minerals revealed the presence of alunogen, antlerite, atacamite, chalcanthite, copiapite, fibroferrite, gypsum, halotrichite, melanterite and pickeringite, being chemically aluminium sulphates, hydrated sulphates of iron aluminium and magnesium aluminium, hydrated copper sulphates, copper hydroxide sulphates and hydroxide chlorides, hydrated iron sulphates, iron hydroxide sulphates with various degrees of hydration and hydrated calcium sulphates. However, some phases such as pyrite, chalcopyrite, quartz, chlorite/clinochlore, mica group minerals, kaolinite, alunite, jarosite and hematite are considered here as substrates due to their presence beneath the previous ones (examples in Figure 3).

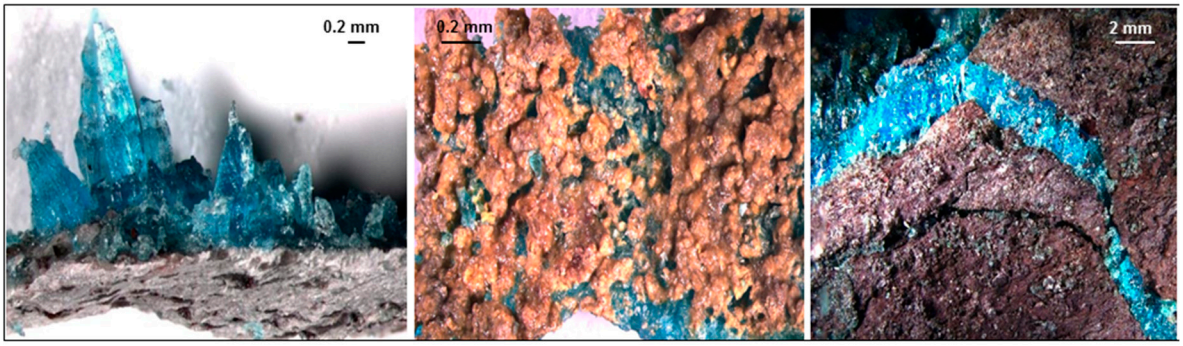

Figure 3. Stereomicroscope images of chalcanthite (blue) over chlorite/clinochlore (volcanic rock, grey), jarosite (brownish) and hematite (reddish), as they occur in the adit wall.

4.1.1. Alunite/Jarosite

Alunite [$(K,Na)Al_3(SO_4)_2(OH)_6$] and jarosite [$KFe_3(SO_4)_2(OH)_6$] belong to the alunite supergroup with general formula $AB_3(SO_4)_2(OH)_6$ (A = K^+, Na^+, plus minor Ag^+, Tl^+, NH^{4+}, Pb^{2+}, Bi^{3+}, and B = Al^{3+} or Fe^{3+}, respectively, in the subgroups of alunite and jarosite) [23]. Massive cryptocrystalline aggregates of yellowish alunite occur associated with quartz and mica (Figure 4a) or associated with hematite and quartz (brownish red). Yellow/brownish jarosite appears with quartz and mica (Figure 4b) or with chlorite/clinochlore + quartz, or even with kaolinite + quatz + pyrite, as a substrate for alunogen, halotrichite/pickeringite, chalcanthite and melanterite.

Table 1. Inventory of the mineralogical phases identified by XRD (alphabetical order) and principal characteristics; data about solubility are from Hammarstrom [22]: s, highly soluble in water; i, relatively insoluble in water; -, non-individualized minerals when observed under the stereomicroscope.

Name	Chemical Formula	Habit	Colour	JCPDF Card Number
Alunite	$(K,Na)Al_3(SO_4)_2(OH)_6$	massive cryptocrystalline aggregates	yellowish	14–136
Alunogen (s)	$Al_2(SO_4)_3{\cdot}17H_2O$	massive macrocrystalline aggregates	white	26–1010
Antlerite (i)	$Cu_3(SO_4)(OH)_4$	massive aggregates	pale green	7–407
Atacamite	$Cu_2Cl(OH)_3$	massive	dark green	25–269
Chalcanthite (s)	$CuSO_4{\cdot}5H_2O$	massive, crystalline, fibrous columnar, crusts	deep or light blue	11–646
Chalcopyrite	$CuFeS_2$	-	-	37–471
Chlorite/Clinochlore	$(Mg,Fe)_5Al_2Si_3O_{10}(OH)_8$	massive	grey	24–506
Copiapite (s)	$Fe^{2+}Fe^{3+}{}_4(SO_4)_6(OH)_2{\cdot}20H_2O$	macro crystalline aggregates	deep yellow	35–583
Fibroferrite	$Fe^{3+}(OH)SO_4{\cdot}5H_2O$	acicular crystals	whitish	83–1803
Gypsum (i)	$CaSO_4{\cdot}2H_2O$	radial aggregates of crystals	white, greyish	33–311
Halotrichite (s)	$FeAl_2(SO_4)_4{\cdot}22H_2O$	aggregates of acicular crystals	white	39–1387
Hematite	α-Fe_2O_3	massive	reddish	33–664
Jarosite (i)	$KFe_3(SO_4)_2(OH)_6$	massive aggregates	brownish	22–827
Kaolinite	$Al_2Si_2O_5(OH)_4$	massive	yellowish	75–938
Melanterite (s)	$FeSO_4{\cdot}7H_2O$	massive, crystalline, fibrous columnar, crusts	greenish, yellow, bluish	22–633
Mica group minerals	$(K,H_3O)Al_2Si_3AlO_{10}(OH)_2$	-	-	26–911
Pyrite	FeS_2	-	-	42–1340
Quartz	α-SiO_2	crystalline	white	46–1045

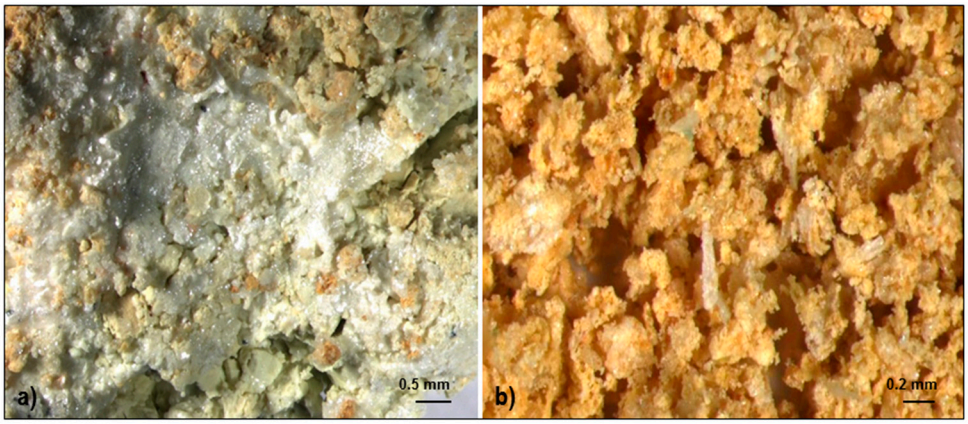

Figure 4. Stereomicroscope images of: (**a**) Alunite; (**b**) jarosite collected in the Algares adit.

4.1.2. Alunogen

Alunogen, $Al_2(SO_4)_3{\cdot}17H_2O$, was frequently found as white crystalline aggregates (Figure 5), occasionally associated with chalcanthite (blue) or with halotrichite/pickeringite, jarosite and melanterite. The translucent crystals appear over quartz, chlorite/clinochlore + quartz or kaolinite + hematite + quartz. In opposition to the common accepted value of 18 water molecules, studies performed by Fang and Robinson [24] showed that the maximum H_2O content in the alunogen formula is 17 molecules.

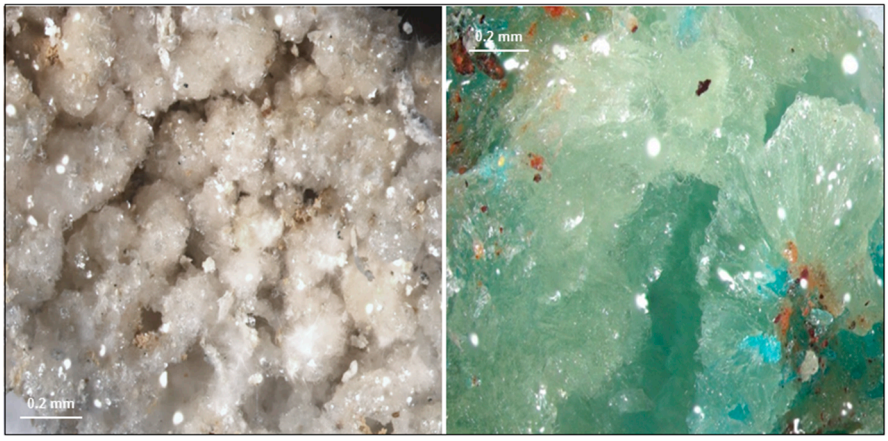

Figure 5. Alunogen (stereomicroscope images) in the Algares adit.

4.1.3. Antlerite

The pale green antlerite (Figure 6), $Cu_3(SO_4)(OH)_4$, is a rare mineral in the adit walls and appears associated with chalcanthite. The massive aggregates of antlerite crystals seem to be associated with an intermediate zone between the reddish substrate (chlorite/clinochlore + hematite + quartz) and the chalcanthite (the presence of chalcanthite probably resulted from the precipitation of later fluids over antlerite).

4.1.4. Atacamite

Dark green atacamite (orthorhombic) or paratacamite (rhombohedral), occurs associated with gypsum (Figure 7) or with halotrichite/pickeringite, over chlorite/clinochlore + mica + quartz, hematite + pyrite or chlorite/clinochlore+hematite. These minerals are polymorphic forms of $Cu_2Cl(OH)_3$.

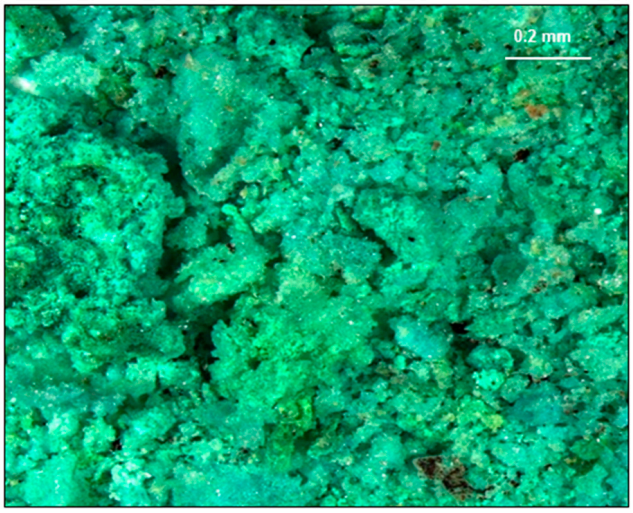

Figure 6. Stereomicroscope image of pale green antlerite.

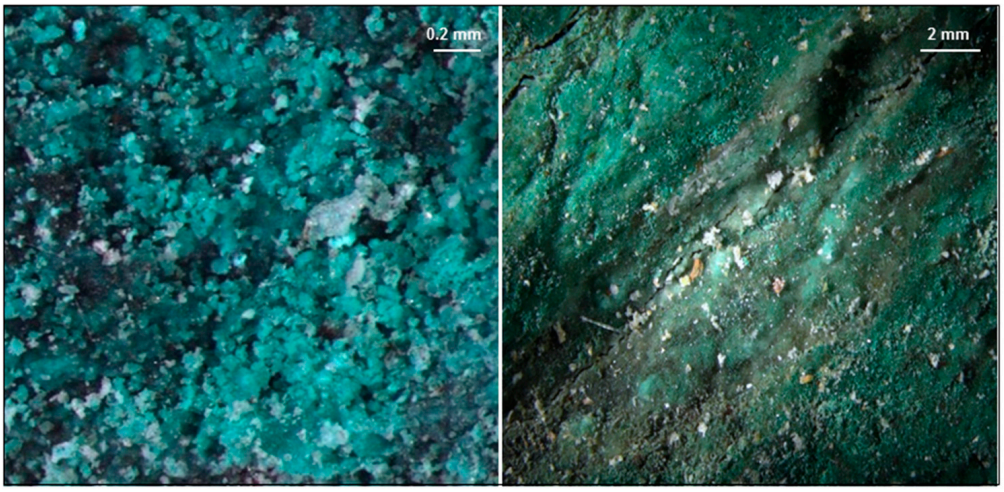

Figure 7. Different aspects of dark green atacamite (stereomicroscope images).

4.1.5. Chalcanthite

Of the blue coloured samples, chalcanthite ($CuSO_4 \cdot 5H_2O$) is the most common mineral found in the adit, changing from vitreous deep blue masses to light blue crystals to fibrous columnar crystalline or crusts, as shown by the stereomicroscope images (Figure 8). The DTA-TG curve performed in one sample of supposedly chalcanthite was compared to published data [25] (p. 122), and the phase constitution of heated material was monitored by XRD. Four endothermic peaks were obtained at about 155, 275, 775 and 830 °C and the resulting material was a mixture of tenorite (CuO) plus cuprite (Cu_2O). These results reflect the chalcanthite decomposition under inert atmosphere.

Chalcanthite occurs associated with almost all minerals identified in the adit walls: Alunogen, gypsum, halotrichite/pickeringite, melanterite, antlerite, fibroferrite; the following minerals were found as substrates: Quartz, chlorite/clinochlore + quartz, hematite + chlorite/clinochlore + quartz, kaolinite + hematite. In the hand specimen, it could be confused with copper-rich melanterite, due to the similar colouration. The general formula of the chalcanthite group is $M^{2+}SO_4 \cdot 5H_2O$, where M = Cu, Fe, Mg, Mn [26]. The structure consists of isolated SO_4 tetrahedra linked to $Cu(H_2O)_6$ octahedra, forming zig-zag infinite chains with composition $Cu(H_2O)_4SO_4$ [27].

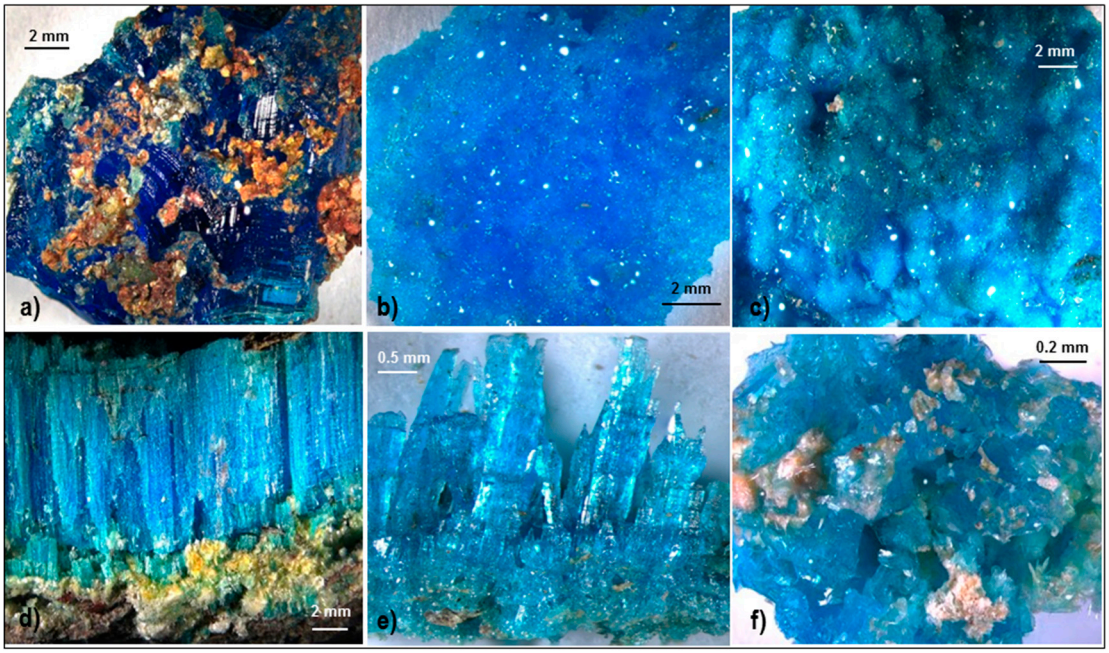

Figure 8. Several aspects of chalcanthite: Vitreous deep blue masses (**a**), light blue crystals (**d**–**f**), fibrous columnar crystalline (**d**) and crusts (**b**,**c**) (stereomicroscope images).

4.1.6. Copiapite

Sulphates of the copiapite group include mixed-valence minerals with general formula $A^{2+}Fe^{3+}{}_4(SO_4)_6(OH)_2{\cdot}20H_2O$, wherein A = Ca, Cu, Fe (copiapite *s.s.*), Mg, Zn, and trivalent minerals with general formula $B^{3+}{}_{2/3}Fe^{3+}{}_4(SO_4)_6(OH)_2{\cdot}20H_2O$, wherein B = Al, Fe [22]. Deep-yellow copiapite (Figure 9) is not abundant in the Algares adit, occurring associated with a small quantity of gypsum in a single sample.

Figure 9. Stereomicroscope image of deep-yellow copiapite.

4.1.7. Fibroferrite

Fibroferrite, $Fe^{3+}(OH)SO_4{\cdot}5H_2O$, is not abundant in the Algares adit. Whitish aggregates of acicular crystals were found over hematite (Figure 10). Fibroferrite is the end-member of the basic iron sulphate series $Fe(OH)SO_4.xH_2O$; the structure contains hydroxo-bridged $\{Fe(OH)(H_2O)_2\ SO_4\}$ spiral chains built of $[Fe(OH)_2(H_2O)_2O_2]$ octahedra and SO_4 tetrahedra, connected by hydrogen bonds [28].

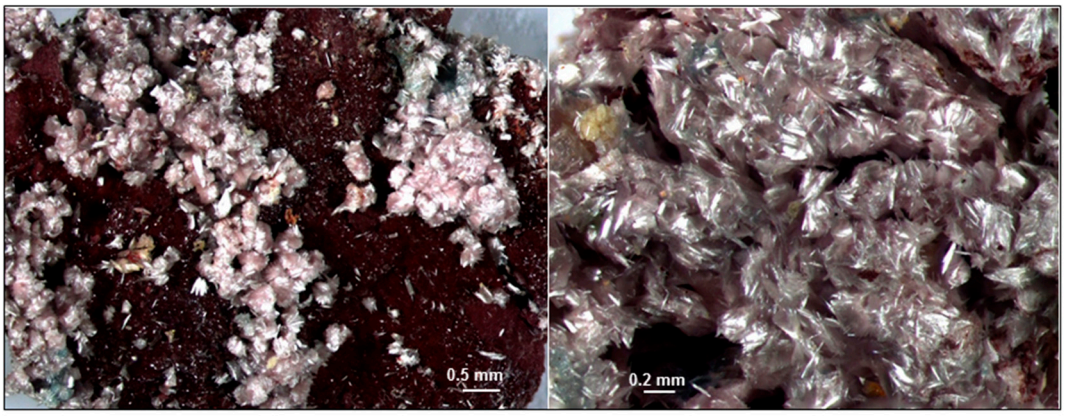

Figure 10. Stereomicroscope images of fibroferrite over hematite.

4.1.8. Gypsum

White or greyish aggregates and crystals of gypsum (Figure 11), $CaSO_4 \cdot 2H_2O$, were frequently found, associated with atacamite or melanterite and sometimes with chalcanthite. The thin and elongated (up to 2 cm) efflorescences of hyaline crystals have a radial shape. The adit sector located SW of the Algares East gossan is full of microcrystalline aggregates of gypsum. These sulphates are present in fine crusts in rock surface of the *Mine Tuff* volcanic rocks which present disseminated sulphide mineralisation. These crystals can show a dark grey colour interpreted as a consequence of dust deposition due to the rehabilitation works performed inside the adit.

Figure 11. Stereomicroscope image of radial aggregates of gypsum in the Algares adit.

4.1.9. Halotrichite/Pickeringite

Sulphates of the halotrichite group have the general formula $AB_2(SO_4)_4 \cdot 22H_2O$, where A = Fe^{2+}, Mg^{2+}, Mn^{2+}, Ni^{2+}, Zn^{2+}, and B = Al^{3+}, Cr^{3+}, Fe^{3+} [22]. There is complete miscibility between Mg^{2+} and Fe^{2+} in the pickeringite-halotrichite series [29]. These sulphates occur as white (mainly) or orange aggregates of fine-acicular crystals (Figure 12). The orange colour in pickeringite can be due to the substitution of Al^{3+} by Fe^{3+} [30]; iron content in these samples increased from about 0.1% (white) to more than 5% (orange). The distinction between halotrichite and pickeringite was achieved through the iron and magnesium contents (Figure 12); really, the ratio Mg/Fe obtained was 0.02 (halotrichite), 7.0 (pickeringite) and 0.2 (ferric-pickeringite). Halotrichite/pickeringite minerals were identified

in mixtures mainly with melanterite, but also with alunogen or chalcanthite, over quartz + pyrite, quartz + hematite, jarosite + quartz or quartz + chlorite/clinochlore + mica.

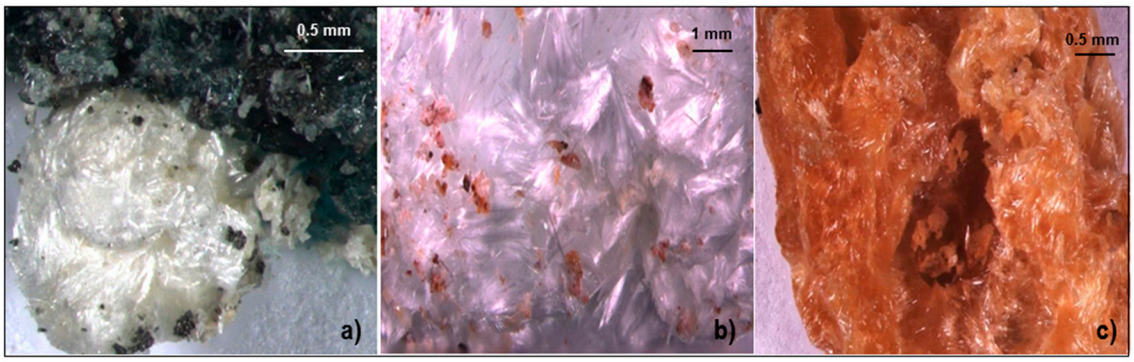

Figure 12. Stereomicroscope images of halotrichite (**a**), pickeringite (**b**) and of the iron-rich pickeringite (**c**).

4.1.10. Melanterite

Melanterite, the heptahydrate iron (II) sulphate, is readily soluble in water and, when exposed to air, tends to lose hydration water and alters to rozenite ($FeSO_4 \cdot 4H_2O$) or to siderotil ($FeSO_4 \cdot 5H_2O$); if melanterite is Cu-rich, it tends to dehydrate to siderotil [22]. From the iron minerals, melanterite ($FeSO_4 \cdot 7H_2O$) is the most common with colours from greenish yellow to bluish (Figure 13) and variable contents of iron/copper/zinc. Although not well-established, it seems that the blue colour is related to copper and, visually, cuprian melanterite can be confused with chalcanthite [31]; the yellow/brownish colouration (Figure 13) could be related to the presence of ferric oxide [22]. Indeed, the general formula of melanterite is $M^{2+}SO_4 \cdot 7H_2O$, where M represents a divalent cation such as Co, Cu, Fe, Mg, Mn and Zn [31]. The crystal structure of melanterite is formed by a SO_4 tetrahedron, two independent $M(H_2O)_6$ octahedra, and one interstitial H_2O group which is not directly bonded to M^{2+} cations (e.g., [32,33]).

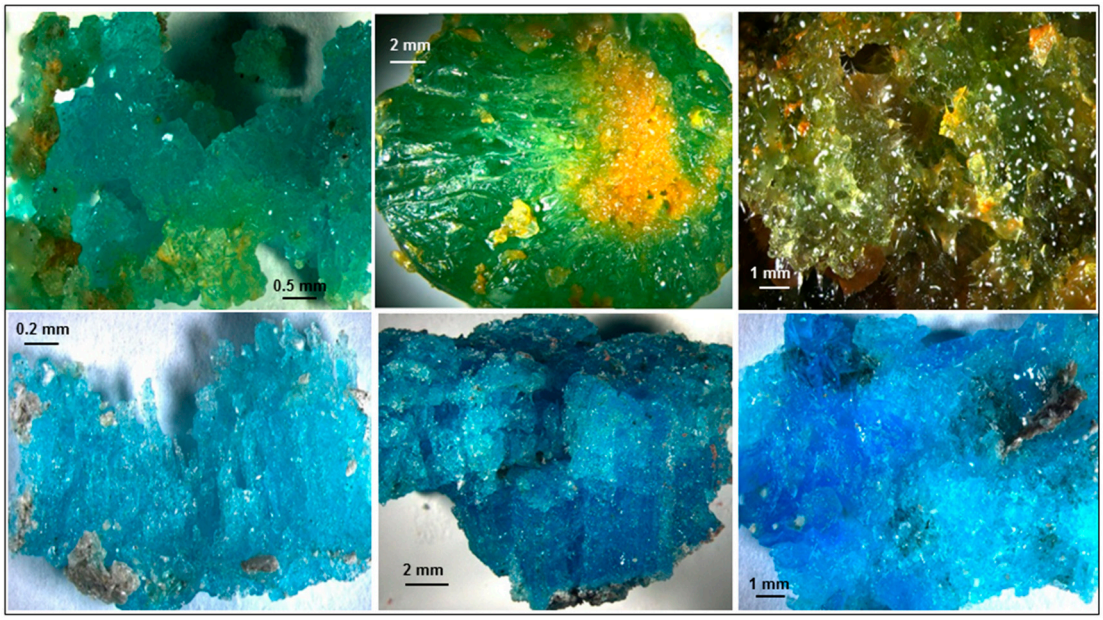

Figure 13. Stereomicroscope images of melanterite.

The green melanterite stalactites/stalagmites in Algares revealed a high content of Fe (>20%), no copper and a small amount of Zn (1–2%); in crusts from the walls, the Cu content increases (5–9%), and one sample presents even 15% Cu. These values are presented in the ternary diagram of Figure 14,

although being only indicative due to the equipment used (portable XRF) and to the presence of vestigial phases. Stalactites were formed closer to an old ore shoot structure inside the adit with percolation of water (see Figure 2). With a cylindrical shape, some tubes are up to 3 cm in length and 0.5 cm in diameter. Below these structures, on the ground, stalagmites with a botryoidal habit have formed, being green outside and yellow inside (due to minute amounts of Fe^{3+}? e.g., [31]). The XRD identification showed only melanterite in both colours of minerals. Melanterite from the walls occurs associated to gypsum, pickeringite, alunogen or chalcanthite, mainly over quartz + pyrite, quartz + chlorite/clinochlore, pyrite + kaolinite. Rozenite and siderotil were not identified in Algares adit, although melanterite is highly soluble in water and tends to lose hydration water.

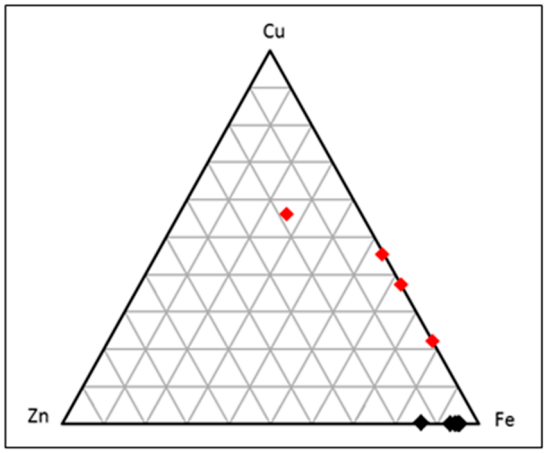

Figure 14. Ternary diagram showing the content of Fe/Cu/Zn in melanterite samples from walls (red) and from stalactites/stalagmites (black).

DTA-TG assays were also performed in three samples of supposedly melanterite, one without copper and the remainder being copper-rich. The sample free of Cu showed endothermic peaks at about 120, 170, 325, 355, 530 (small peak) and 770 °C, in accordance to published data [25] (p. 123). The decomposition under inert atmosphere gave rise to magnetite (Fe_3O_4) and hematite, reflecting the previous existence of melanterite. The DTA-TG curves of the two samples with Cu were similar, with endothermic peaks at about 100, 160, 350, 720, 775 and 815 °C, and the formation of magnetite plus tenorite, compatible with a former Cu-rich melanterite.

As an historical reference, a pigment, known as "Azul de Aljustrel" (Aljustrel Blue), was described in a document from King John III (16th century) and referred to as being produced in Aljustrel by a regal functionary, refined and sold to artists [34]. The use of "Azul de Aljustrel" pigment is thought to have been an episode lasting only a few years, as no other references are known [35]. Concerning its nature, it is supposed that it might have been a pigment based on copper sulphates or basic copper carbonates existing in the sulphur deposits of the Aljustrel region [36]. In similar deposits in the Spanish IPB, ancient references about the collection of materials in pits for making paint and for medicinal use (probably in Rio Tinto) led Rebollar [37] to consider that these materials were sulphates and melanterite rather than chalcanthite.

In the case of the Algares adit, melanterite stalactites and stalagmites are located below the old ore silo opening on the roof of the adit. In fact, above the gallery, crushed massive sulphide ore is still present, and through the air flow and rainwater percolation, the precipitation of sulphates occurs in the mine adit roof and floor.

5. Discussion

Indeed, the great majority of the minerals identified (Table 1) are frequently found in acid mine drainage (AMD) environments (e.g., [38–42]) and, depending on their solubility and environmental

conditions, could be visible on the ground. Some of them are already mentioned as occurring in mill tailings impoundments from Algares [43]. Other authors also refer their presence as a coating of the gallery walls (e.g., [37,44–46]), being long preserved from dissolution.

Melanterite ($FeSO_4 \cdot 7H_2O$) and chalcanthite ($CuSO_4 \cdot 5H_2O$) are the most common minerals found in the Algares adit; covering the walls, they appear associated with almost all secondary minerals and over the majority of substrates. Melanterite from the walls revealed to be Cu-rich by opposition to that from stalactites/stalagmites formed below the old ore storage silo (see Section 4.1.10). This can be explained by the expected Cu supergene enrichment observed in the mine adit and the presence of low-copper-grade ores exploited underground and stored in the mine silo. Dehydration of melanterite was not observed, as the species rozenite and siderotil were not identified, revealing that the temperature and humidity of the adit favour melanterite stability. On the other hand, copiapite [$Fe^{2+}Fe^{3+}{}_4(SO_4)_6(OH)_2 \cdot 20H_2O$] was found only in one efflorescent sample, representing an advanced stage in the oxidation sequence.

Indeed, the oxidation of primary Fe and Cu sulphide minerals (pyrite, FeS_2 and chalcopyrite, $CuFeS_2$)—see the possible reaction pathways in Hammarstrom [22], Parafiniuk [47], Bigham and Nordstrom [48]—give rise to the formation of Fe^{2+} and Cu^{2+} salts (secondary sulphate minerals), namely melanterite and chalcanthite, respectively, or even hematite (depending on relative humidity and time [49]). Occurrences of melanterite have been reported, for example, at Rio Tinto (Spain) [38]; Falun (Sweden) [26]; Apuan Alps, Tuscany (Italy) [32]; or even at Genna Luas, Sardinia (Italy). In the last locality, melanterite was pointed out not only as the result of pyrite weathering, but also the precursor of copiapite [50]. Chalcanthite is commonly found in the late stage oxidation zones of copper deposits or on mine walls by the action of acidic surface waters on copper veins (e.g., as in Rio Tinto, Spain [37]). Due to its ready solubility in water, it tends to crystallise, dissolve and recrystallise as crusts depending on the humidity conditions. Copiapite forms from the precipitation of iron salts in mixed valence (2+, 3+), is frequently found with other sulphates and was considered one of the earliest basic minerals originating from the oxidation of pyrite ores [51].

Furthermore, an aqueous solution of Fe^{2+}/Mg^{2+} combined with Al^{3+} from silicates give rise to halotrichite [$FeAl_2(SO_4)_4 \cdot 22H_2O$]/pickeringite [$MgAl_2(SO_4)_4 \cdot 22H_2O$]. In the Algares adit, these sulphates occur as white (mainly) or orange aggregates of crystals. According to the ratio Mg/Fe obtained (see Section 4.1.9), the orange colour in pickeringite can be due to the substitution of Al^{3+} by Fe^{3+} [30]. Pickeringite crystals (white, creamy or light pink) were found as efflorescences on the surface of weathered schists, associated with the decomposition of chlorite (Mg source) through acidic solutions derived from the oxidation of pyrite [52]. Halotrichite/pickeringite minerals were identified in the adit in mixtures, sometimes with another aluminium sulphate, the alunogen [$Al_2(SO_4)_3 \cdot 17H_2O$] (this one frequently found as white crystalline aggregates along the walls). Alunogen is formed by the actions of sulphate solutions resulting from the oxidation of the sulphides on aluminous minerals and is found in the wall rock of pyritic ore deposits [26] or in salt efflorescence from AMD (e.g., [53]).

Besides chalcanthite, other copper minerals identified were antlerite [$Cu_3(SO_4)(OH)_4$] (rarely found in the adit walls) and atacamite [$Cu_2Cl(OH)_3$] (occurring associated with gypsum or with halotrichite/pickeringite). Antlerite usually appears in the oxidised zones of copper ore veins in the arid areas such as Chuquicamata Mine in Chile, and in several deposits in Arizona, USA [26,54]. The crystallisation of antlerite from solution probably occurs at 30–35 °C, as shown by experiments concerning antlerite stability [54]. Atacamite and paratacamite are polymorphs; while the first one seems to be more stable at room temperature, the second one is formed in solutions of relatively low $CuCl_2$ concentration [55]. Atacamite is an important constituent of supergene oxide zones of copper deposits in the Atacama Desert of northern Chile, and its formation is related to gypsum-saturated saline groundwaters [56,57].

White or greyish aggregates and crystals with a radial shape of gypsum ($CaSO_4 \cdot 2H_2O$) were frequently found in the Algares gallery, while fibroferrite [$Fe^{3+}(OH)SO_4 \cdot 5H_2O$] is not abundant and found over hematite. The occurrence of both minerals in pyrite-bearing schists has been described by, e.g., Parafiniuk [47,52].

Alunite [(K,Na)$Al_3(SO_4)_2(OH)_6$]/jarosite [$KFe_3(SO_4)_2(OH)_6$] forms in extremely acidic environments by the hydrolysis of Al^{3+}/Fe^{3+} when combined with K^+ from silicates. Alunite veins from the Algares deposit were already studied and correlated with the kaolinite [$Al_2Si_2O_5(OH)_4$] supergene alteration along the gossan [9–11]. In the Algares adit, alunite veins are present in small late fractures over the stockwork veins areas. They are located near the Algares West gossan, close to the old roman galleries that occur in the upper part of the gallery. In consequence of the great geotechnical instability observed in the gallery, some sections near the gossans developed above the massive ore are protected by concrete walls. These protections do not allow observation near gossan oxides and sulphate mineral assemblages.

Kaolinite [$Al_2Si_2O_5(OH)_4$], from the kaolin group, and illite [$(K,H_3O)Al_2Si_3AlO_{10}(OH)_2$], the general term used here for mica group, are clay minerals formed by the chemical weathering of aluminium-bearing silicate minerals. They occur as substrates of sulphate minerals. The occurrence of the kaolinite/halloysite supergene alteration is referred to the Algares gossan, showing a clear zonation and high intensity near the ore lenses [9–11]. This clay alteration zoning is related to supergene processes and can achieve up to >40 m depth. According to these authors, the same alteration occurs in the IPB Lagoa Salgada, Lousal, Caveira and São Domingos deposits.

Chemistry of Sulphate Minerals

The oxidation of sulphide minerals in metallic ore deposits, with the generation of acidic solutions, usually leads to the formation of both insoluble and water-soluble, metal-bearing sulphates, hydroxysulphates, as found in the present work (Table 1). Summarising, variations in the compositions of the soluble metal-sulphate salts found in the Algares adit allow separation into the following groups of minerals, according to Jambor [58]: (1) Simple hydrated salts with divalent cations, of the type $M^{2+}SO_4{\cdot}nH_2O$, n = 7, 5, 2: Melanterite, chalcanthite and gypsum; (2) simple hydrated salts with trivalent cations, characterised by the general formula $A_2(SO_4)_3{\cdot}nH_2O$, where A is Fe^{3+} or Al—only alunogen was found; (3) mixed divalent–trivalent sulphate salts, with the general formula $AR_2(SO_4)_2.nH_2O$, where A = Mg, Fe^{2+}, and R = Al, Fe^{3+}: Halotrichite, pickeringite—in that category, Jambor [58] also includes the OH-bearing copiapite, $Fe^{2+}Fe^{3+}{}_4(SO_4)_6(OH)_2{\cdot}20H_2O$; (4) complex salts—anhydrous sulphates containing hydroxyl of the type $A_m(SO_4)_p(OH)_q$, namely, antlerite, and of the type $A_2(SO_4)(OH)_q$, specifically, alunite and jarosite; and (5) the complex, hydrated sulphate salt, fibroferrite, $Fe^{3+}(SO_4)(OH){\cdot}5H_2O$. Concerning the occurrence of the metal atom, chalcanthite and melanterite are clearly the main copper and iron sulphates, respectively, while alunogen and pickeringite dominate the aluminium sulphates.

6. Conclusions

The massive sulphides and stockwork mineralisation hosted by the *Mine Tuff* volcanic rocks unit in the Algares adit show intense supergene alteration, but the sheltered environment of this underground mine gallery provides the preservation of water-soluble minerals. The continuous air flow and constant humidity are favourable conditions for mineral precipitation occurring as complex mineral assemblages. The abundance, variety and chemical composition of minerals (mostly sulphates) are essentially linked with the chemical composition of the ores (mainly pyrite and chalcopyrite). In that way, melanterite ($FeSO_4{\cdot}7H_2O$) and chalcanthite ($CuSO_4{\cdot}5H_2O$) were the most commonly observed minerals on the multi-coloured aggregates, resulting from the weathering through acidic waters; these minerals were found essentially as massive or crystalline aggregates, with colours ranging from greenish to bluish. The difference observed in copper content of melanterite samples collected on stalactites/stalagmites (copper-free) and adit walls (up to 15% Cu) can be explained by the expected Cu supergene enrichment observed in the walls and the presence of low-copper-grade ores exploited underground and stored in the old Algares mine silo. Although the species rozenite and siderotil were not identified, revealing that the temperature and humidity favour melanterite

stability, copiapite [$Fe_5(SO_4)_6(OH)_2{\cdot}20H_2O$] was found in one sample, indicating an advanced stage in the oxidation sequence.

Aqueous solution of Fe^{2+}/Mg^{2+} combined with Al^{3+} from silicates gave rise to other mixed divalent–trivalent sulphate salts as halotrichite [$FeAl_2(SO_4)_4{\cdot}22H_2O$]/pickeringite [$MgAl_2(SO_4)_4{\cdot}22H_2O$]. Pickeringite also occurs in samples with an orange colour (iron content of more than 5% and ratio of Mg/Fe of 0.2) probably related to the substitution of Al^{3+} by Fe^{3+}.

Well-developed whitish crystals of gypsum ($CaSO_4{\cdot}2H_2O$) were easily recognised, but, while in the form of aggregates, they can be confused with other white minerals such as alunogen [$Al_2(SO_4)_3{\cdot}17H_2O$], or with crystals of fibroferrite [$Fe^{3+}(OH)SO_4{\cdot}5H_2O$], halotrichite or pickeringite. Yellowish minerals found in the walls can be alunite [$(K,Na)Al_3(SO_4)_2(OH)_6$] or kaolinite [$Al_2Si_2O_5(OH)_4$], and when brownish, jarosite [$KFe_3(SO_4)_2(OH)_6$], or even copiapite. Besides chalcanthite, other copper species were identified: Antlerite (rare) [$Cu_3(SO_4)(OH)_4$], a pale green mineral; and deep-green atacamite [$Cu_2Cl(OH)_3$], whose presence is indicative of the percolation of saline fluids. These minerals intercalated/over chlorite/clinochlore (grey) or hematite (reddish) give the adit a rainbow colour effect, making this an attractive mining heritage site to visit.

Author Contributions: Conceptualization, T.P.S., J.X.M., D.D.O. and J.P.V.; methodology, T.P.S. and J.P.V.; investigation, T.P.S., J.X.M., D.D.O., J.P.V., I.M. and P.G.; writing—original draft preparation, T.P.S., J.X.M. and D.D.O.; writing—review and editing, T.P.S., J.X.M., D.D.O., J.P.V., I.M., P.G. and L.A.; visualization, T.P.S.; funding acquisition, J.X.M., J.P.V. All authors have read and agreed to the published version of the manuscript.

Funding: Funding from EDM Company and FEDER (*Fundo Europeu de Desenvolvimento Regional*)/INTERREG POCTEP GEO-FPI- (Ref. 0052-GEO-FPI-5-E) and EXPLORA, Op ALT20-03-0145-FEDER-000025, funded by Alentejo 2020, Portugal 2020 and European Union (ERDF) is acknowledged. J.P. Veiga acknowledges FEDER funds through the COMPETE 2020 Programme and National Funds through FCT-Portuguese Foundation for Science and Technology under the project UID/CTM/50025/2019, and the funding from the European Institute of Innovation and Technology (EIT), a body of the European Union, under the Horizon 2020, the EU Framework Programme for Research and Innovation, through the MineHeritage Project (PA 18111).

Acknowledgments: Thanks are due to Fernanda Carvalho for performing the chemical analysis through XRF-WDS. We are also grateful to Ana Rita Silva and Marta Silva for focus stacking the stereomicroscope images. Special thanks are also due to the anonymous reviewers for their comments on the manuscript.

Conflicts of Interest: The authors declare no conflict of interest.

References

1. Barriga, F.J.A.S.; Carvalho, D.; Ribeiro, A. Introduction to the Iberian Pyrite Belt. In *Geology and VMS Deposits of the Iberian Pyrite Belt*; Society of Economic Geologists: Littleton, CO, USA, 1997; Volume 27, pp. 1–20.
2. Almodóvar, G.R.; Yesares, L.; Sáez, R.; Toscano, M.; González, F.; Pons, J.M. Massive sulfide ores in the Iberian Pyrite Belt: Mineralogical and textural evolution. *Minerals* **2019**, *9*, 653. [CrossRef]
3. Matos, J.X.; Martins, A.; Rego, M.; Mateus, A.; Pinto, A.; Figueiras, J.; Silva, E. Roman Slag Distribution in the Portuguese Sector of the Iberia Pyrite Belt. In *Actas of the "V Congreso Internacional sobre Minería y Metalurgia Históricas en el Suroeste Europeo (León 2008)"*; Mata-Perelló, J.M., Iabat, L.T., Prieto, M.N.F., Eds.; SEDPGYM: Madrid, Spain, 2011; pp. 567–576.
4. Matos, J.X.; Martins, L.P.; Oliveira, J.T.; Pereira, Z.; Batista, M.J.; Quental, L. Pyrite Route in the Portuguese Sector of the Iberian Pyrite Belt, Challenges for a Sustained Development of Geological Tourism and Mining. In *Rutas Minerales en Iberoamérica*; Carrion, P., Ed.; Escuela Superior Politécnica del Litoral: Guayaquil, Equador, 2008; pp. 136–155. (In Portuguese)
5. Matos, J.X. Expansion and Development of the Pyrite Route through the inclusion of the Geological Gardens of Algares and Lousal, Iberian Pyirite Belt, Portugal. In *Rutas Minerales en Iberoamérica*; Carrion, P., Ed.; Escuela Superior Politécnica del Litoral: Guayaquil, Equador, 2009; pp. 113–121. (In Portuguese)
6. Andrade, R.F. The mine of Aljustrel. *Bol. Minas* **1967**, *4*, 73–90. (In Portuguese)
7. Andrade, R.; Schermerhorn, L. Aljustrel and Gavião. In *Livro Guia da Excursão 4. I Congresso Hipano-Luso-Americano de Geologia Económica*; Carvalho, D., Goinhas, J., Schermerhorn, L.J.S., Eds.; Direcção-Geral de Minas e Serviços Geológicos: Lisbon, Portugal, 1971; pp. 32–59.

8. Matos, J.X.; Martins, L.P. Environmental rehabilitation of mining areas in the Portuguese sector of the Iberian Pyrite Belt: State of the art and future perspectives. *Boletín Geológico Min.* **2006**, *117*, 289–304. (In Portuguese)
9. Matos, J.X.; Barriga, F.; Oliveira, V. Alunite veins versus supergene kaolinite-halloysite alteration in the Lagoa Salgada, Algares and S. João, Aljustrel, and S. Domingos massive sulphide deposits, Iberian Pyrite Belt, Portugal. In Proceedings of the VI Congresso Nacional de Geologia, Caparica, Portugal, 4–6 June 2003; pp. B56–B59.
10. Matos, J.X.; Barriga, F.J.A.S.; Relvas, J.M.R.S. Acid Sulphate Alteration in the Iberian Pyrite Belt. In Proceedings of the 14th SGA Biennial Meeting, Mineral Resources to Discover, Quebec City, QC, Canada, 20–23 August 2017; Volume II, pp. 625–628.
11. Matos, J.X.; Barriga, F.J.A.S.; Relvas, J.M.R.S. Acid Sulphate Alteration at the Lagoa Salgada, Aljustrel and São Domingos VMS Deposits, Iberian Pyrite Belt, Portugal: Mineral Exploration Guidelines. *Geophys. Res. Abstr.* **2019**, *21*, EGU2019-9641-1.
12. Brilha, J.; Andrade, C.; Azerêdo, A.; Barriga, F.J.A.S.; Cachão, M.; Couto, H.; Cunha, P.P.; Crispim, J.A.; Dantas, P.; Duarte, L.V.; et al. Definition of the Portuguese frameworks with international relevance as an input for the European geological heritage characterization. *Episodes* **2005**, *28*, 177–186. [CrossRef]
13. Matos, J.X.; Pereira, Z. The LNEG ATLANTERRA South Portuguese Zone Geosite characterization Program. In Proceedings of the 11th European Geoparks Conference, Arouca, Portugal, 19–21 September 2012; Sá, A., Rocha, D., Paz, A., Correia, V., Eds.; AGA—Associação Geoparque Arouca: Arouca, Portugal, 2012; pp. 189–190.
14. Silva, T.P.; Matos, J.X.; De Oliveira, D.; Morais, I.; Gonçalves, P.; Albardeiro, L.; Veiga, J.P. Mineralogical Characterization of the Algares 30-level Adit for Cultural Tourism, Aljustrel Mine, Iberian Pyrite Belt. In *Book of Abstracts of "Materiais 2019"*; Rectorate of the NOVA University of Lisbon: Lisbon, Portugal, 2019; p. 353.
15. Leitão, J. Geology of the Aljustrel Massive Sulfides Deposits. *Seg Guideb. Ser. V* **1997**, *27*, 82–97.
16. Leitão, J. Geology of the Massive Sulphide Deposits of Aljustrel. In *Livro Guia das Excursões do V Congresso Nacional de Geologia*; IGM-Instituto Geológico e Mineiro: Lisbon, Portugal, 1998; pp. 91–100. (In Portuguese)
17. Luís, A.T.; Durães, N.; Silva, E.F.; Ribeiro, S.; Silva, A.J.F.; Patinha, C.; Almeida, S.F.P.; Azevedo, M.R. Tracking multiple Sr sources through variations in $^{87}Sr/^{86}Sr$ ratios of surface waters from the Aljustrel massive sulphide mining area: Geological versus anthropogenic inputs. *Appl. Geochem.* **2019**, *102*, 108–120. [CrossRef]
18. Gaspar, O.C. Microscopy and petrology of ores applied to the genesis, exploration and mineralogy of the massive sulphides of the Aljustrel and Neves-Corvo deposits. *Estud. Notas E Trab. Inst. Geológico E Min.* **1996**, *38*, 3–195. (In Portuguese)
19. Schermerhorn, L.; Zbyzewski, G.; Ferreira, V. *Notícia Explicativa da Carta Geológica 42D Aljustrel*; SGP: Lisbon, Portugal, 1987; p. 55.
20. Rosa, D.; Finch, A.; Andersen, T.; Inverno, C. U–Pb geochronology and Hf isotope ratios of magmatic zircons from the Iberian Pyrite Belt. *Min. Pet.* **2009**, *95*, 47–69. [CrossRef]
21. Matos, J.X.; Pereira, Z.; Fernandes, P.; Rosa, D.; Oliveira, J.T. Contribution to the understanding of the structure of Aljustrel mine Iberian Pyrite Belt, based in new palynostratigraphical data obtained in the Volcano-Sedimentary Complex and Mértola Formation. *VIII Congr. Nac. De Geol. E Terra* **2010**, *21*, 1–4. (In Portuguese)
22. Hammarstrom, J.M.; Seal, R.R., II; Meier, A.L.; Kornfeld, J.M. Secondary sulfate minerals associated with acid drainage in the eastern US: Recycling of metals and acidity in surficial environments. *Chem. Geol.* **2005**, *215*, 407–431. [CrossRef]
23. Stoffregen, R.E.; Alpers, C.N.; Jambor, J.L. Alunite-Jarosite Crystallography, Thermodynamics, and Geochronology. In *Reviews in Mineralogy and Geochemistry, Sulfate Minerals-Crystallography, Geochemistry, and Environmental Significance*; Alpers, C.N., Jambor, J.L., Nordstrom, D.K., Eds.; Mineralogical Society of America: Chantilly, VA, USA, 2000; Volume 40, pp. 453–479.
24. Fang, J.H.; Robinson, P.D. Alunogen, $Al_2(H_2O)_{12}(SO_4)3.5H_2O$; its atomic arrangement and water content. *Am. Min.* **1976**, *61*, 311–317.
25. Földvári, M. *Handbook of Thermogravimetric System of Minerals and Its Use in Geological Practice*; Kiadó, F., Ed.; Geological Institute of Hungary: Budapest, Hungary, 2011.
26. Palache, C.; Berman, H.; Frondel, C. *Dana's System of Mineralogy*, 7th ed.; John Wiley & Sons, Inc.: Hoboken, NJ, USA, 1951; Volume II.

27. Lima-de-Faria, J. *Structural Mineralogy—An Introduction*; Kluwer Academic Publishers: Dordrecht, The Netherlands, 1994; p. 317.
28. Scordari, F. Fibroferrite: A mineral with a $\{Fe(OH)(H_2O)_2SO_4\}$ spiral chain and its relationship to $Fe(OH)SO_4$, butlerite and parabutlerite. *TMPM Tschermaks Petr. Mitt.* **1981**, *28*, 17–29. [CrossRef]
29. Menchetti, S.; Sabelli, C. The halotrichite group: The crystal structure of apjohnite. *Min. Mag.* **1976**, *40*, 599–608. [CrossRef]
30. Parafiniuk, J.; Siuda, R.; Borkowski, A. Sulphate and arsenate minerals as environmental indicators in the weathering zones of selected ore deposits, Western Sudetes, Poland. *Acta Geol. Pol.* **2016**, *66*, 493–508. [CrossRef]
31. Peterson, R.C. The relationship between Cu content and distortion in the atomic structure of melanterite from the Richmond mine, Iron Mountain, California. *Can. Mineral.* **2003**, *41*, 937–949. [CrossRef]
32. Mauro, D.; Biagioni, C.; Pasero, M. Crystal-chemistry of sulfates from Apuan Alps (Tuscany, Italy). I. Crystal structure and hydrogen bond system of melanterite, $Fe(H_2O)_6(SO_4)\cdot H_2O$. *Period. Mineral.* **2018**, *87*, 89–96. [CrossRef]
33. Baur, W.H. On the crystal chemistry of salt hydrates. III. The determination of the crystal structure of $FeSO_4\cdot 7H_2O$ (melanterite). *Acta Crystallogr.* **1964**, *17*, 1167–1174. [CrossRef]
34. Município de Aljustrel. History of Mining, Câmara Municipal de Aljustrel. Available online: http://www.mun-aljustrel.pt/menu/114/historiada-mineracao.aspx (accessed on 23 April 2020). (In Portuguese)
35. Cruz, A.J. The Provenance of the Pigments used in Painting in Portugal Before the Invention of Paint Tubes: Problems and Perspectives. In *As Preparações na Pintura Portuguesa. Séculos XV e XVI*; Serrão, V., Antunes, V., Seruya, A.I., Eds.; Faculty of Letters/Lisbon University: Lisbon, Portugal, 2013; (In Portuguese). [CrossRef]
36. Gil, M.; Seruya, A.I.; Aguiar, J.; Candeias, A.; Frade, J.C.; Valadas, S.; Alves, P.; Ribeiro, I. Colored limewash paintings in Alentejo (Part 1): Pigments' identification and stratigraphic analysis (in 2004–2006). *Conservar Património* **2009**, *10*, 19–38. (In Portuguese) [CrossRef]
37. Rebollar, M.C.; Díaz, F.G.; Oliá, J.V. Mineralogy of the Iberian Pyrite Belt. *Bocamina* **1999**, *4*, 50–85. (In Spanish)
38. Buckby, T.; Black, S.; Coleman, M.L.; Hodson, M.E. Fe-sulphate-rich evaporative mineral precipitates from the Rio Tinto, southwest Spain. *Min. Mag.* **2003**, *67*, 263–278. [CrossRef]
39. Nieto, J.M.; Sarmiento, A.M.; Olías, M.; Canovas, C.R.; Riba, I.; Kalman, J.; Delvalls, T.A. Acid mine drainage pollution in the Tinto and Odiel rivers (Iberian Pyrite Belt, SW Spain) and bioavailability of the transported metals to the Huelva Estuary. *Environ. Intern.* **2007**, *33*, 445–455. [CrossRef] [PubMed]
40. Sánchez-España, J. Acid mine drainage in the Iberian Pyrite Belt: An overview with special emphasis on generation mechanisms, aqueous composition and associated mineral phases. *Macla* **2008**, *10*, 34–43.
41. Abreu, M.M.; Batista, M.J.; Magalhães, M.C.F.; Matos, J.X. Acid Mine Drainage in the Portuguese Iberian Pyrite Belt. In *Mine Drainage and Related Problems*; Robinson, B.C., Ed.; Nova Science Publishers, Inc.: Hauppauge, NY, USA, 2010; pp. 71–118.
42. Gallo, A.A. Mineralogía y Geoquímica de Sulfatos Secundarios en Ambientes de Drenaje Ácido de Mina. Área Minera del Yacimiento de San Miguel (Faja Pirítica Ibérica). Ph.D. Thesis, Universidad del País Vasco, Leioa, Spain, October 2010; p. 273.
43. Bobos, I.; Durães, N.; Noronha, F. Mineralogy and geochemistry of mill tailings impoundments from Algares (Aljustrel), Portugal: Implications for acid sulfate mine waters formation. *J. Geochem. Explor.* **2006**, *88*, 1–5. [CrossRef]
44. Alpers, C.N.; Nordstrom, D.K.; Thompson, J.M. Seasonal Variations of Zn/Cu Ratios in Acid Mine Water from Iron Mountain, California. In *Environmental Geochemistry of Sulfide Oxidation*; ACS Symposium Series 550; Alpers, C.N., Blowes, D.W., Eds.; American Chemical Society: Washington, DC, USA, 1993; pp. 324–344.
45. De Waele, J.; Forti, P. Mineralogy of Mine Caves in Sardinia (Italy). In Proceedings of the 14th International Congress of Speleology, Kalamos, Greece, 21–28 August 2005; pp. 306–311.
46. Verhaert, M.; Bernard, A.; Saddiqi, O.; Dekoninck, A.; Essalhi, M.; Yans, J. Mineralogy and genesis of the polymetallic and polyphased low grade Fe-Mn-Cu ore of Jbel Rhals deposit (Eastern High Atlas, Morocco). *Minerals* **2018**, *8*, 23. [CrossRef]
47. Parafiniuk, J. Sulfate minerals and their origin in the weathering zone of the pyrite-bearing schists at Wiesciszowice (Rudawy Janowickie Mts, Western Sudetes). *Acta Geol. Pol.* **1996**, *46*, 353–414.

48. Bigham, J.M.; Nordstrom, D.K. Iron and Aluminium Hydroxysulfates from Acid Sulfate Waters. In *Reviews in Mineralogy and Geochemistry, Sulfate Minerals-Crystallography, Geochemistry, and Environmental Significance*; Alpers, C.N., Jambor, J.L., Nordstrom, D.K., Eds.; Mineralogical Society of America: Chantilly, VA, USA, 2000; Volume 40, pp. 351–403.
49. Borek, S.L. Effect of Humidity on Pyrite Oxidation. In *Environmental Geochemistry of Sulfide Oxidation*; ACS Symposium Series 550; Alpers, C.N., Blowes, D.W., Eds.; American Chemical Society: Washington, DC, USA, 1993; pp. 31–44.
50. Frau, F. The formation-dissolution-precipitation cycle of melanterite at the abandoned pyrite mine of Genna Luas in Sardinia, Italy: Environmental implications. *Min. Mag.* **2000**, *64*, 995–1006. [CrossRef]
51. Fanfani, L.; Nunzi, A.; Zanazzi, P.F.; Zanzari, A.R. The copiapite problem: The crystal structure of a ferrian copiapite. *Am. Min.* **1973**, *58*, 314–322.
52. Parafiniuk, J. Fibroferrite, slavikite and pickeringite from the oxidation zone of pyrite-bearing schists in Wiesciszowice (Lower Silesia). *Min. Pol.* **1991**, *22*, 3–15.
53. Valente, T.; Grande, J.A.; Torre, M.L. Magnesium and Aluminium Sulfates in Salt Efflorescences from Acid Mine Drainage in the Iberian Pyrite Belt (SW Spain). In Proceedings of the IMWA 2016, Leipzig, Germany, 11–15 July 2016; Drebenstedt, C., Paul, M., Eds.; Technische Universität Bergakademie Freiberg: Freiberg, Germany, 2016; pp. 445–450.
54. Pollard, A.M.; Thomas, R.G.; Williams, P.A. The stabilities of antlerite and $Cu_3SO_4(OH)_4{\cdot}2H_2O$: Their formation and relationships to other copper(II) sulfate minerals. *Min. Mag.* **1992**, *56*, 359–365. [CrossRef]
55. Fleet, M.E. The crystal structure of paratacamite, $Cu_2(OH)_3Cl$. *Acta Cryst.* **1975**, *B31*, 183–187. [CrossRef]
56. Cameron, E.M.; Leybourne, M.I.; Palacios, C. Atacamite in the oxide zone of copper deposits in northern Chile: Involvement of deep formation waters? *Min. Depos.* **2007**, *42*, 205–218. [CrossRef]
57. Reich, M.; Palacios, C.; Parada, M.A.; Fehn, U.; Cameron, E.M.; Leybourne, M.I.; Zúñiga, A. Atacamite formation by deep saline waters in copper deposits from the Atacama Desert, Chile: Evidence from fluid inclusions, groundwater geochemistry, TEM, and ^{36}Cl data. *Min. Depos.* **2008**, *43*, 663–675. [CrossRef]
58. Jambor, J.L.; Nordstrom, D.K.; Alpers, C.N. Metal-sulfate Salts from Sulfide Mineral Oxidation. In *Reviews in Mineralogy and Geochemistry, Sulfate Minerals-Crystallography, Geochemistry, and Environmental Significance*; Alpers, C.N., Jambor, J.L., Nordstrom, D.K., Eds.; Mineralogical Society of America: Chantilly, VA, USA; Volume 40, pp. 303–350.